Journal for ImmunoTherapy of Cancer

CXCL10 and Nrf2-upregulated mesenchymal stem cells reinvigorate T lymphocytes for combating glioblastoma

Jiaji Mao,[1] Jianing Li,[1] Junwei Chen,[1] Qin Wen,[1] Minghui Cao,[1] Fang Zhang,[1] Baoxun Li,[1] Qinyuan Zhang,[1] Zhe Wang,[1] Jingzhong Zhang,[2] Jun Shen [1]

To cite: Mao J, Li J, Chen J, *et al*. CXCL10 and Nrf2-upregulated mesenchymal stem cells reinvigorate T lymphocytes for combating glioblastoma. *Journal for ImmunoTherapy of Cancer* 2023;**11**:e007481. doi:10.1136/jitc-2023-007481

► Additional supplemental material is published online only. To view, please visit the journal online (http://dx.doi.org/10.1136/jitc-2023-007481).

JM and JL contributed equally.

Accepted 19 November 2023

[1]Department of Radiology, Guangdong Provincial Key Laboratory of Malignant Tumor Epigenetics and Gene Regulation, Sun Yat-Sen Memorial Hospital, Sun Yat-Sen University, Guangzhou, Guangdong, China
[2]The Key Laboratory of Bio-Medical Diagnostics, Suzhou Institute of Biomedical Engineering and Technology, Suzhou, Jiangsu, China

Correspondence to
Dr Jun Shen;
shenjun@mail.sysu.edu.cn

ABSTRACT

Background Lack of tumor-infiltrating T lymphocytes and concurrent T-cell dysfunction have been identified as major contributors to glioblastoma (GBM) immunotherapy resistance. Upregulating CXCL10 in the tumor microenvironment (TME) is a promising immunotherapeutic approach that potentially increases tumor-infiltrating T cells and boosts T-cell activity but is lacking effective delivery methods.

Methods In this study, mesenchymal stem cells (MSCs) were transduced with a recombinant lentivirus encoding *Cxcl10*, *Nrf2* (an anti-apoptosis gene), and a ferritin heavy chain (*Fth*) reporter gene in order to increase their CXCL10 secretion, TME survival, and MRI visibility. Using FTH-MRI guidance, these cells were injected into the tumor periphery of orthotopic GL261 and CT2A GBMs in mice. Combination therapy consisting of CXCL10-Nrf2-FTH-MSC transplantation together with immune checkpoint blockade (ICB) was also performed for CT2A GBMs. Thereafter, in vivo and serial MRI, survival analysis, and histology examinations were conducted to assess the treatments' efficacy and mechanism.

Results CXCL10-Nrf2-FTH-MSCs exhibit enhanced T lymphocyte recruitment, oxidative stress tolerance, and iron accumulation. Under in vivo FTH-MRI guidance and monitoring, peritumoral transplantation of CXCL10-Nrf2-FTH-MSCs remarkably inhibited orthotopic GL261 and CT2A tumor growth in C57BL6 mice and prolonged animal survival. While ICB alone demonstrated no therapeutic impact, CXCL10-Nrf2-FTH-MSC transplantation combined with ICB demonstrated an enhanced anticancer effect for CT2A GBMs compared with transplanting it alone. Histology revealed that peritumorally injected CXCL10-Nrf2-FTH-MSCs survived longer in the TME, increased CXCL10 production, and ultimately remodeled the TME by increasing $CD8^+$ T cells, interferon-γ^+ cytotoxic T lymphocytes (CTLs), $GzmB^+$ CTLs, and Th1 cells while reducing regulatory T cells (Tregs), exhausted $CD8^+$ and exhausted $CD4^+$ T cells.

Conclusions MRI-guided peritumoral administration of CXCL10 and Nrf2-overexpressed MSCs can significantly limit GBM growth by revitalizing T lymphocytes within TME. The combination application of CXCL10-Nrf2-FTH-MSC transplantation and ICB therapy presents a potentially effective approach to treating GBM.

WHAT IS ALREADY KNOWN ON THIS TOPIC

⇒ Glioblastoma (GBM) immunotherapy resistance has been linked primarily to a deficiency in tumor-infiltrating T cells and concurrent T-cell dysfunction. A promising immunotherapy strategy for GBM involves using mesenchymal stem cells (MSCs) to deliver CXCL10, which may improve tumor-infiltrating T cells and restore T-cell activity in the tumor microenvironment (TME); nevertheless, the limited survival of transplanted MSCs in GBM poses a substantial challenge.

WHAT THIS STUDY ADDS

⇒ CXCL10 could be used to revive T cells in immunologically "distinct" GBM, and overexpressing Nrf2 in MSCs is an effective method for boosting MSC survival in order to function as cellular vehicles for CXCL10 delivery to GBM. Besides, FTH-MRI is a practical method for guiding intracranial stem cell transplantation. Peritumoral CXCL10-Nrf2-FTH-MSC implantation effectively inhibited the growth of intracranial GL261 and CT2A GBMs and extended animal survival. The capacity of CXCL10-Nrf2-FTH-MSCs to restore T-cell dysfunction could be augmented when combined with immune checkpoint blockade therapy for CT2A GBM.

HOW THIS STUDY MIGHT AFFECT RESEARCH, PRACTICE OR POLICY

⇒ Peritumoral administration of CXCL10 and Nrf2-overexpressed MSCs can substantially inhibit the growth of GBM by reinvigorating T lymphocytes within the TME. Combining CXCL10-Nrf2-FTH-MSC transplantation with immune checkpoint blockade therapy can potentially be a more effective treatment regimen for GBM than either alone.

BACKGROUND

Glioblastoma (GBM) is the most prevalent and severe type of brain tumor, accounting for almost half of all primary central nervous system (CNS) malignancies.[1] Despite improvements in surgical resection, radiotherapy, chemotherapy, and recently

proposed targeted therapy or tumor-treating fields, GBM remains notorious for its dismal prognosis, with a median survival of less than 2 years and an exceptionally low 5-year survival rate (<10%).[2 3]

Immunotherapy, which employs the host's immune system to combat cancer, has made significant clinical advances in a broad range of malignancies over the past decade, and this has also spurred intensive research into its potential use for GBM.[4] Although there have been numerous immunotherapeutic clinical trials, such as immune checkpoint blockade (ICB), chimeric antigen receptor T (CAR T) cell therapy, and oncolytic virotherapy, for the treatment of GBM, very few have shown a substantial improvement in survival.[5] Complex mechanisms are underneath. A lack of tumor-infiltrating lymphocytes and contemporaneous T-cell dysfunction have been recognized as key contributors to treatment resistance in GBM among the multifactorial factors.[6] Hence, it is extremely desirable to recruit effector T lymphocytes to the tumor site and unleash their full potential. CXCL10 could not only facilitate the migration of T cells to the tumor site but also drive their polarization into highly potent effector T cells.[7 8] Increasing the level of CXCL10 in the tumor microenvironment (TME) is therefore a prospective method for GBM immunotherapy. Nevertheless, CXCL10 has a very short half-life in blood,[9] making it difficult to reach therapeutic levels in the brain without causing systemic side effects through systemic administration. Furthermore, in order to enhance tumor-infiltrating T cells and restore T-cell functionality in GBM, continuous and high-level CXCL10 delivery is necessary, which is also challenging to achieve via systemic administration.

Recently, tumoricidal stem cells have created an immunotherapy avenue for GBM.[10] Using genetically modified stem cells to deliver high, sustained concentrations of tumoricidal agents such as immunotherapeutic cytokines and oncolytic viruses locally to primary or recurrent GBM could overcome the limitations of current systemic chemotherapy approaches.[11] In a completed phase I clinical trial, intracranial administration of neural stem cells carrying an engineered oncolytic adenovirus to patients with high-grade gliomas after tumor removal was shown to be safe, and it elicited an anti-glioma immune response, with promising survival outcomes for GBM.[12] Compared with other types of stem cells, the lack of immunogenicity and the simplicity of obtaining and expanding mesenchymal stem cells (MSCs) without raising ethical concerns make them attractive cellular vehicles for treating GBM.[13] Our previous study demonstrated that peritumorally injected interferon (IFN)-β gene-modified MSCs (IFN-β-MSCs) significantly inhibit intracranial malignant glioma growth, as evidenced by their longer survival compared with intracerebral, intratumoral, and intra-arterial injections, indicating that peritumoral injection is the preferred administration route for MSC-based cellular vehicles.[14] On day 11 after peritumoral injection, however, the survival rate of IFN-β-MSCs engrafted in the glioma periphery is still only about 30%. The limited survival of engrafted MSCs remains a significant barrier to their therapeutic efficacy. Thus, improving MSC survival in the TME is essential for increasing their therapeutic utility. Gliomas develop an aberrant vasculature network and an altered redox microenvironment characterized by variable oxygen concentrations and elevated amounts of reactive oxygen species (ROS),[15] which are highly detrimental to MSC survival. The *NFE2L2* gene, which encodes Nrf2, is a stress-responsive transcription factor that is essential for the cellular response to a variety of stressors, such as oxidative damage and senescence, an excessive supply of nutrients and metabolites, inflammation, etc.[16] Several studies have shown that Nrf2 overexpression enhances MSC survival and oxidative stress tolerance,[17 18] which could be used to improve the effectiveness of MSC-based cell therapies.

In the present research, MSCs were transduced with a lentivirus carrying *Cxcl10*, *Nrf2*, and the ferritin heavy chain (*Fth*) reporter gene in order to enhance their CXCL10 secretion, Nrf2 expression, and MRI visibility. These MSCs were implanted into the tumor periphery of orthotopic GL261 and CT2A GBM in mice under FTH-based MR guidance. CT2A GBMs were also treated with combination therapy combining CXCL10-Nrf2-FTH-MSC transplantation and ICB. Subsequently, in vivo and serial MRI, survival analysis, and histology tests were conducted to assess the efficacy and therapeutic mechanisms of different treatments. This research aims to determine whether Nrf2-upregulated MSCs could be employed for continuous and targeted delivery of CXCL10 to increase tumor-infiltrating T cells, restore their function in GBM, and restrict GBM progression.

METHODS

Lentiviral vector construction and MSC transduction

MSCs derived from C57BL/6 mice were obtained from PROCELL Life Technology (Wuhan, China). Lentiviral vectors encoding mouse *Cxcl10* (NM_021274), *Fth* (NM_010239), and enhanced green fluorescent protein (*eGFP*) with or without *Nrf2* (NM_010902), or encoding *Nrf2* and *eGFP* were constructed (LV-CXCL10-T2A-Nrf2-P2A-FTH-eGFP, LV-CXCL10-T2A-FTH-eGFP, and LV-Nrf2-eGFP). MSCs were transduced with LV-CXCL10-T2A-Nrf2-P2A-FTH-eGFP, and genetically modified MSCs (CXCL10-Nrf2-FTH-MSCs) were obtained. CXCL10-FTH-MSCs, Nrf2-MSCs, and eGFP-MSCs were obtained by transducing MSCs with LV-CXCL10-T2A-FTH-eGFP, LV-Nrf2-eGFP, or the lentiviral vector encoding eGFP alone as controls. The Methods section of the online supplemental materials included details on lentiviral vector construction and MSC transduction.

Cytotoxicity and effectiveness testing in vitro

To evaluate the safety of lentivirus transduction, as previously described,[14] flow cytometry (FCM) and the CCK8 assay were used to evaluate the phenotype of genetically modified MSCs and cell viability. The messenger RNA

(mRNA) overexpression of *Cxcl10*, *Nrf2*, and *Fth* in genetically modified MSCs was detected using quantitative real-time PCR (qPCR). ELISA was used to confirm the over-secretion of CXCL10 in genetically modified MSCs, and western blot was used to confirm the overexpression of Nrf2 and FTH. The transwell migration assay was used to assess the effect of CXCL10 over-secretion on the ability of CXCL10-Nrf2-FTH-MSCs to recruit T cells. The ability of Nrf2 overexpression to protect CXCL10-Nrf2-FTH-MSCs from ROS was evaluated using H_2O_2-induced cell apoptosis. FCM was employed to detect apoptosis in genetically modified MSCs with and without H_2O_2 preconditioning. As previously described,[14] Prussian blue (PB) staining and in vitro MRI were used to evaluate the overexpression of the *Fth* gene in CXCL10-Nrf2-FTH-MSCs. The in vitro MRI sequence acquisition parameters are provided in the online supplemental table 1. The CCK8 assay and FCM were employed to evaluate the viability and apoptosis of GL261 cells co-cultured with CXCL10-Nrf2-FTH-MSCs in order to detect the direct cytotoxicity of CXCL10 over-secretion against GBM cells. FCM was used to determine the effect of CXCL10-Nrf2-FTH-MSCs on T-cell phenotype by analyzing the phenotype of T cells co-cultured with CXCL10-Nrf2-FTH-MSCs. Details of all the above-mentioned experiments are provided in the online supplemental methods.

Establishment of intracranial orthotopic GL261 and CT2A GBM models and MSC delivery

PROCELL Life Technology (Wuhan, China) provided the GL261 cells. BeNa Culture Collection (Beijing, China) provided the CT2A cells. From the Guangdong Province Medical Experimental Animal Center (Guangzhou, China), adult male C57/BL6 mice weighing 20–30 g were purchased. The individual mouse was considered the experimental unit within the studies. Random numbers were generated using the standard=RAND() function in Microsoft Excel. Immunocompetent C57BL/6 mice were stereotaxically injected with 3×10^5 syngeneic GL261 GBM cells or 0.5×10^5 syngeneic CT2A cells into the left striatum in order to establish orthotopic intracranial GBM models. Four to 7 days following tumor cell inoculation, in vivo MRI was used to confirm GBM establishment. Details of intracranial orthotopic GBM establishment are provided in the online supplemental methods.

Mice bearing GL261 tumors were randomly divided into five experimental groups and received one of the five treatments, including peritumoral injection of 2×10^6 CXCL10-Nrf2-FTH-MSCs, CXCL10-FTH-MSCs, Nrf2-MSCs, eGFP-MSCs, or PBS, when tumor burden reached $3\pm1\,mm^3$ on MRI T2WI. Once the CT2A tumor burden measured by MRI T2WI was $2\pm1\,mm^3$, mice were given one of five treatments: peritumoral injection of 2×10^6 CXCL10-Nrf2-FTH-MSCs combined with ICB by intraperitoneal injection of an anti-mouse programmed cell death-1 (PD-1) antibody, as previously described[19 20] (CXCL10-Nrf2-FTH-MSC + ICB group), peritumoral injection of 2×10^6 CXCL10-Nrf2-FTH-MSCs (CXCL10-Nrf2-FTH-MSC group), intraperitoneal injection of an anti-mouse PD-1 antibody (ICB group), peritumoral injection of 2×10^6 CXCL10-Nrf2-FTH-MSCs combined with T-cell depletion by intraperitoneal injection of anti-mouse CD4 and anti-mouse CD8a antibodies, as previously described[21 22] (CXCL10-Nrf2-FTH-MSC + T-cell depletion group), or peritumoral PBS injection (PBS group). An MRI-guided injection of MSCs into the peritumoral zone of orthotopic GBMs was performed, as described in our previous study.[14] Details are elaborated on in the online supplemental methods.

In vivo MRI

In vivo and serial MRI was performed to monitor the therapeutic effect of peritumoral transplantation of MSCs on orthotopic GBMs. MRI was performed on a clinical 3.0 T MR scanner (Ingenia; Philips Medical Systems) equipped with a 3 cm 8-channel phased array mouse coil (Suzhou Zhongzhi Medical Technologies, China). For GL261 tumors (n=5 in each group), in vivo MRI was performed at each time point of 1-day prior to injection (baseline), the day of injection (day 1), and 7, 14, and 21 days after injection (day 1, day 7, day 14, and day 21). CXCL10-Nrf2-FTH-MSCs were identified on T2*W images on day 1 to confirm the peritumoral transplantation. Considering that CT2A tumors often reach end-stage earlier than GL261 tumors, in vivo MRI was performed on CT2A GBM (n=5 in each group) 1-day prior to injection (baseline), 6 and 11 days after injection (day 6 and day 11). The online supplemental table 2, provide the in vivo MRI sequence acquisition parameters. The tumor volume of GBMs in each group at each time point was measured on T2W images, as previously mentioned.[14] The maximum size of the tumors allowed to grow in the mice before euthanasia was $300\,mm^3$.

Survival analysis

Mice bearing GL261 tumors were randomly assigned to one of five groups: CXCL10-FTH-Nrf2-MSC, CXCL10-FTH-MSC, Nrf2-MSC, eGFP-MSC, or PBS (n=6 in each group) in order to assess the impact of CXCL10-Nrf2-FTH-MSCs on animal survival. Mice bearing CT2A tumors were randomly assigned to one of five groups: CXCL10-Nrf2-FTH-MSC + ICB, CXCL10-Nrf2-FTH-MSC, ICB, CXCL10-Nrf2-FTH-MSC + T-cell depletion, and PBS groups (n=6 in each group) in order to assess the effect of CXCL10-Nrf2-FTH-MSCs in combination with ICB or T-cell depletion on animal survival. Each group's animals' survival time was recorded. When animals showed clinical signs of moribund (including serious movement problems, neurological dysfunction, and hunchback), the mice were euthanized.

Histological analysis

The brains of mice bearing GL261 tumors were collected for histologic examination on days 1, 7, and 21 (n=3 per time point in each group). The engraftment of transplanted MSCs was assessed by PB staining and

immunohistochemical labeling for FTH, as previously mentioned.[14] Using a confocal microscope (LSM-880; Zeiss, Jena, Germany), the percentage of eGFP-positive ($eGFP^+$) cells was counted to determine the survival rate of the grafted MSCs. To investigate the impact of transplanted CXCL10-Nrf2-FTH-MSCs on the proliferation and apoptosis of GL261 GBM, immunohistochemical staining for Ki-67 and the TUNEL assay were performed 7 and 21 days after MSC transplantation, respectively. Details are provided in the online supplemental methods.

Ex vivo ELISA and ex vivo FCM

The brains of GL261 tumor-bearing mice were harvested on days 7 and 21 (n=3 at each time point in each group) for ELISA analysis to determine the CXCL10 level in the MSC-transplanted mouse brain. GL261 tumor-bearing mice (n=5 at each time point in each group) were sacrificed on day 7 and day 21 for ex vivo FCM, and mouse brains and deep cervical lymph nodes (dCLNs) were collected to evaluate immune cell infiltration in the tumor and dCLNs following various treatments. To further elucidate the therapeutic mechanism in a mouse model that more closely resembles human GBMs,[23 24] on day 11, ex vivo FCM was performed on the brains of CT2A tumor-bearing mice (n=5 at each time point in each group). For the analysis, 100,000 events were collected for each sample. In the forward scatter/side scatter (FSC/SSC) plots, cells of interest were chosen based on their size. For GL261 tumors, $CD3^+$ cell counts were performed to determine the total number of T cells in the mouse brains. $CD4^+$ and $CD8^+$ T cells were gated within $CD3^+$ T lymphocytes, and immune-activated $CD8^+$ T cells (IFN-γ^+CD8^+ T and $GzmB^+CD8^+$ T cells) were analyzed within $CD8^+$ T cells, while antitumor Th1 cells (IFN-$\gamma^+IL4^-CD4^+$ T cells) and protumor regulatory T cells (Tregs, $CD25^+Foxp3^+CD4^+$ T cells) were gated within $CD4^+$ T cells. $CD45^+$ lymphocytes harboring $CXCR3^+$ cells were gated in dCLNs and mouse brains. Furthermore, for CT2A tumors (n=5 in each group), exhausted $CD8^+$ T lymphocytes (PD-1^+Tim-3^+CD8^+ T cells), exhausted $CD4^+$ T lymphocytes (PD-1^+Tim-3^+CD4^+ T cells), M1 macrophages ($CD86^+CD11b^+F4/80^+CD45^+$) and M2 macrophages ($CD206^+CD11b^+F4/80^+CD45^+$) were also analyzed. Additional information is provided in the online supplemental figure S1.

Statistical analysis

The data are presented as means with SD. mRNA and protein levels, cell viability, apoptosis rate, T-cell migration rate, ex vivo CXCL10 secretion level, and percentage of $eGFP^+$ MSCs and immune cells were compared using one-way analysis of variance, followed by the Bonferroni post hoc test for multiple pairwise comparisons among different times. Using repeated measures analysis of variance, the tumor volume was analyzed. The p values for the Kaplan-Meier survival studies were determined using a log-rank (Mantel-Cox) test. SPSS V.26.0 software was used to conduct statistical analysis (SPSS; Chicago, Illinois, USA). P value<0.05 was considered to indicate a statistically significant difference.

RESULTS

The constructed lentivirus safely transduced MSCs to upregulate CXCL10 secretion, Nrf2, and FTH expression

The schematic of the lentiviral vector employed in this study is depicted in figure 1A. Recombinant lentiviruses LV-CXCL10-T2A-Nrf2-P2A-FTH-eGFP, LV-CXCL10-T2A-FTH-eGFP, and LV-Nrf2-eGFP had a titer of 3×10^8 TU/mL. Following selection with puromycin, the transduction efficiency of both CXCL10-Nrf2-FTH-MSCs, CXCL10-FTH-MSCs, and Nrf2-MSCs increased significantly, with efficiencies of 80.69±0.78%, 73.52±1.31%, and 89.13±0.49%, respectively, compared with 73.47±0.58%, 51.35±0.45%, and 61.86±0.70% in the absence of puromycin selection. Remarkable green fluorescence was observed in CXCL10-Nrf2-FTH-MSCs, CXCL10-FTH-MSCs, and Nrf2-MSCs (figure 1B). Both CXCL10-Nrf2-FTH-MSCs, CXCL10-FTH-MSCs, and Nrf2-MSCs were highly positive for the MSC markers CD44 and CD29, while being negative for the hematopoietic marker CD117 (figure 1C). Furthermore, there were no statistically significant differences in cell viability between CXCL10-Nrf2-FTH-MSCs, CXCL10-FTH-MSCs, eGFP-MSCs, Nrf2-MSCs, and wild-type MSCs (WT-MSCs), as measured by the CCK8 assay (p>0.05) (figure 1D). As determined by qPCR (figure 1E), ELISA (figure 1F), and western blotting (figure 1G), increased expression of CXCL10, Nrf2, and FTH was observed in CXCL10-Nrf2-FTH-MSCs compared with the control groups (p<0.05). Additionally, CXCL10-FTH-MSCs exhibited increased expression of CXCL10 and FTH compared with eGFP-MSCs and WT-MSCs (p<0.05), while Nrf2-MSCs showed higher expression of Nrf2 in comparison to CXCL10-FTH-MSCs, eGFP-MSCs, and WT-MSCs (p<0.001).

CXCL10-Nrf2-FTH-MSCs enhanced T lymphocyte migration, oxidative stress resistance, and cellular iron accumulation

As indicated by the transwell assay, CXCL10-Nrf2-FTH-MSCs and CXCL10-FTH-MSCs significantly increased T-cell migration, particularly $CD8^+$ T-cell migration, compared with Nrf2-MSCs, eGFP-MSCs, WT-MSCs and PBS (p<0.05) (figure 2A). In the H_2O_2-induced apoptosis experiment, the apoptosis rate in the CXCL10-Nrf2-FTH-MSCs and Nrf2-MSCs was only slightly increased by about 8.18% and 8.15%, respectively, whereas the apoptosis rates in the other three groups were significantly upregulated compared with the apoptosis rates of the same cells under normal growth conditions, increasing by approximately 87.57%–89.22% (p<0.001) (figure 2B). These findings suggest that overexpression of Nrf2 improves MSC resistance to oxidative stress. In PB staining, a proportion of CXCL10-Nrf2-FTH-MSCs and CXCL10-FTH-MSCs incubated with iron citrate (Fc) showed abundant blue staining, whereas the other groups did not (figure 2C). After Fc incubation, in vitro MRI demonstrated that

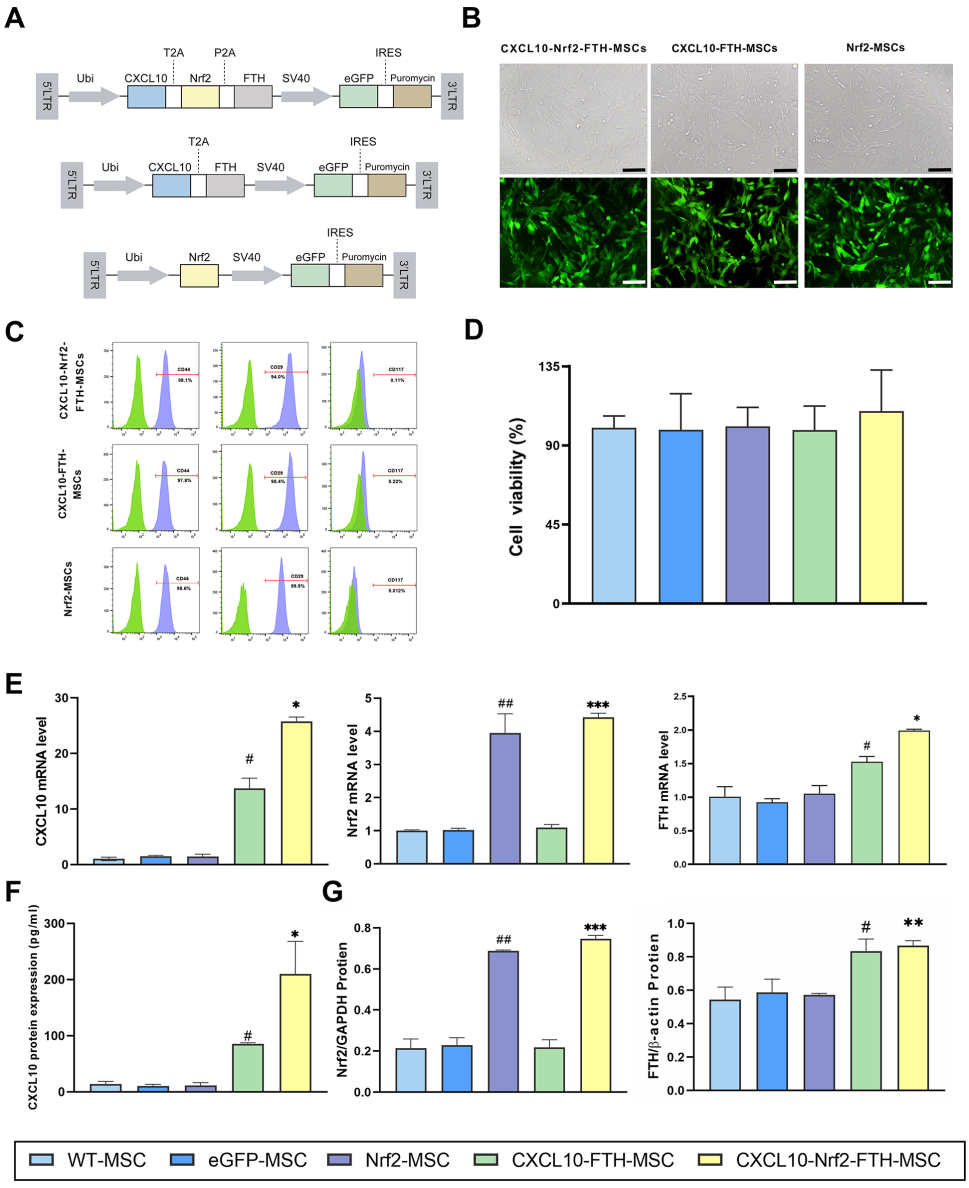

Figure 1 Safety and efficacy of MSC transduction. (A) The schematic of the constructed lentiviral vector. (B) MSCs transfected with CXCL10-T2A-Nrf2-P2A-FTH, CXCL10-T2A-FTH, and Nrf2 overexpressing lentiviruses displayed green fluorescence under phase contrast and inverted fluorescence microscopy. (Bar=100 µm) (C) CXCL10-Nrf2-FTH-MSCs, CXCL10-FTH-MSCs, and Nrf2-MSCs were substantially positive for the MSC markers CD44 and CD29 but negative for the hematopoietic marker CD117, as shown by representative flow cytometric graphs. (D) Graphs demonstrating that there are no statistically significant differences in cell viability between CXCL10-Nrf2-FTH-MSCs, CXCL10-FTH-MSCs, eGFP-MSCs, Nrf2-MSCs, and WT-MSCs. (E) CXCL10-Nrf2-FTH-MSCs showed considerably greater mRNA levels of CXCL10, Nrf2, and FTH than CXCL10-FTH-MSCs, eGFP-MSCs, and WT-MSCs, according to quantitative real-time PCR. CXCL10 secretion and Nrf2 and FTH protein levels in CXCL10-Nrf2-FTH-MSCs were significantly higher than in the other three groups, as assessed by ELISA (F) and western blot (G). ($^{\#}$: CXCL10-FTH-MSCs vs Nrf2-MSCs, eGFP-MSCs, PBS, $p<0.05$; *: CXCL10-Nrf2-FTH-MSCs vs CXCL10-FTH-MSCs, Nrf2-MSCs, eGFP-MSCs, PBS, $p<0.05$; **: CXCL10-Nrf2-FTH-MSCs vs Nrf2-MSCs, eGFP-MSCs, PBS, $p<0.05$; $^{\#\#}$: Nrf2-MSCs vs CXCL10-FTH-MSCs, eGFP-MSCs, WT-MSCs, $p<0.05$; ***: CXCL10-Nrf2-FTH-MSCs vs CXCL10-FTH-MSCs, eGFP-MSCs, WT-MSCs, $p<0.05$). eGFP, enhanced green fluorescent protein; MSCs, mesenchymal stem cells; mRNA, messenger RNA; WT, wild type.

CXCL10-Nrf2-FTH-MSCs and CXCL10-FTH-MSCs had a hypointense signal on T2WI and T2*WI, with a significantly lower signal than the other groups (figure 2D).

After co-cultivation of CXCL10-Nrf2-FTH-MSCs, CXCL10-FTH-MSCs, Nrf2-MSCs, eGFP-MSCs, or WT-MSCs with GL261 cells, respectively, CCK8 and apoptosis assays revealed no statistically significant differences between groups in cell viability and apoptosis rate (figure 2E) ($p>0.05$). The findings demonstrate that CXCL10-Nrf2-FTH-MSCs have no direct effect on the viability and apoptosis rate of GL261 GBM cells. After co-cultivation of CXCL10-Nrf2-FTH-MSCs, CXCL10-FTH-MSCs, Nrf2-MSCs, or eGFP-MSCs with T cells, respectively, FCM revealed that CXCL10-Nrf2-FTH-MSC and

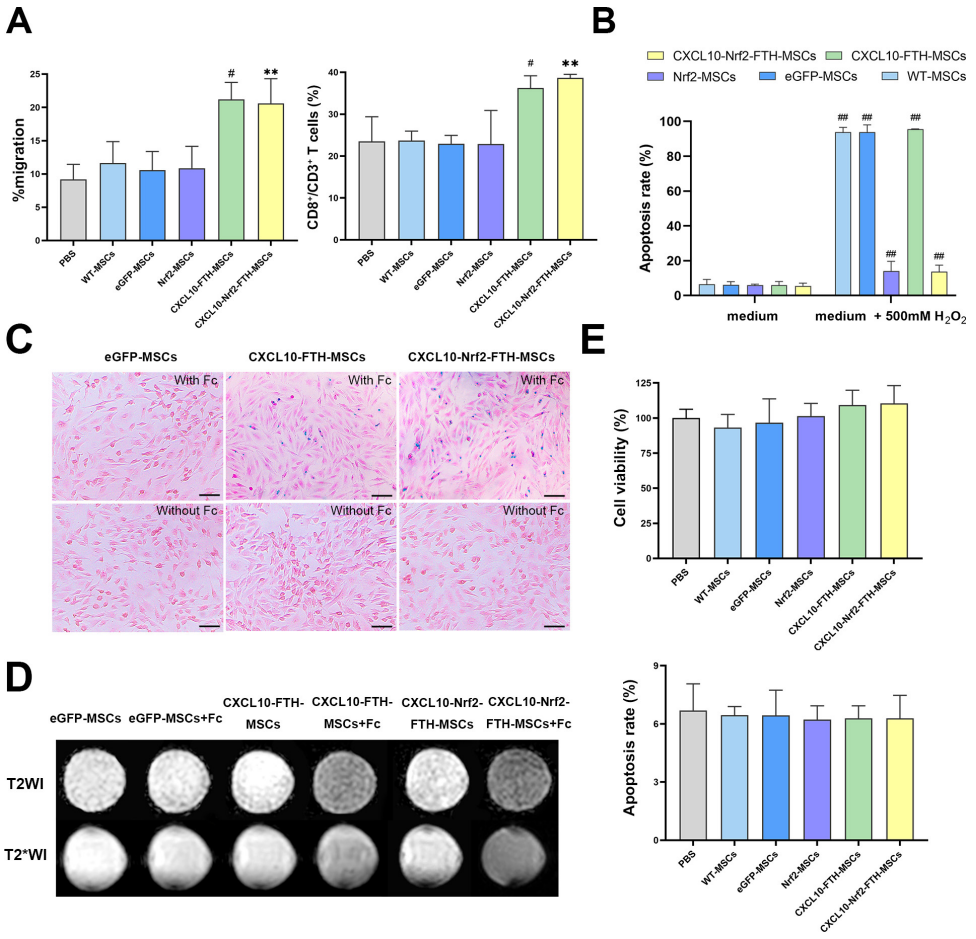

Figure 2 In vitro evaluation of MSCs overexpressing CXCL10, Nrf2, and FTH. (A) The transwell assay revealed that CXCL10-Nrf2-FTH-MSCs and CXCL10-FTH-MSCs significantly improved T-cell migration, especially $CD8^+$ T-cell migration, compared with Nrf2-MSCs, eGFP-MSCs, and WT-MSCs, as shown by flow cytometry. (B) Experiments on H_2O_2-induced apoptosis revealed that the apoptosis rates of CXCL10-Nrf2-FTH-MSCs and Nrf2-MSCs increased by only 8% following H_2O_2 treatment, whereas the apoptosis rates of the other three groups increased by around 90%. (C) Representative micrographs of cell Prussian blue staining reveal abundant blue-stained particles within CXCL10-Nrf2-FTH-MSCs and CXCL10-FTH-MSCs with Fc treatment, but negligible blue-stained particles within CXCL10-Nrf2-FTH-MSCs and CXCL10-FTH-MSCs without Fc treatment, or in eGFP-MSCs with or without Fc incubation (bar=100 µm). (D) On T2W and T2*W images, CXCL10-Nrf2-FTH-MSCs and CXCL10-FTH-MSCs treated with Fc exhibited an evidently hypointense signal. (E) CCK8 and apoptosis experiments revealed no statistically significant differences in proliferation and apoptosis rate between CXCL10-Nrf2-FTH-MSCs, CXCL10-FTH-MSCs, Nrf2-MSCs, and eGFP-MSCs. ($^{\#}$: CXCL10-FTH-MSCs vs Nrf2-MSCs, eGFP-MSCs, WT-MSCs, PBS, $p<0.05$; **: CXCL10-Nrf2-FTH-MSCs vs Nrf2-MSCs, eGFP-MSCs, WT-MSCs, PBS, $p<0.05$; $^{\#\#}$: cells under normal growth conditions vs cells under medium added with 500 mM H_2O_2, $p<0.05$). eGFP, enhanced green fluorescent protein; MSCs, mesenchymal stem cells; WT, wild type.

CXCL10-FTH-MSC groups had a higher percentage of Th1 cells compared with other groups ($p<0.01$) (online supplemental figure S2). There were no other significant differences in T-cell phenotype across the groups ($p>0.05$).

MRI-guided peritumoral transplantation of CXCL10-Nrf2-FTH-MSC inhibits GL261 and CT2A GBM growth

Peritumoral MSC transplantation is illustrated in online supplemental figure S3, as verified by MRI and histological examinations. At baseline, GL261 tumors exhibited a mass with a somewhat hyperintense signal and were frequently bordered by hypointense hemorrhage on T2*W images. On D01, CXCL10-Nrf2-FTH-MSCs and CXCL10-FTH-MSCs presented hypointense signals on T2*W imaging at the peritumoral zone. This is consistent with an abundance of FTH-positive and blue-stained MSCs shown on immunohistochemistry staining for FTH and PB staining, as well as an abundance of $eGFP^+$ cells in the peritumoral area seen on eGFP immunofluorescence imaging. In contrast, no hypointense signal was detected on T2*W images of the eGFP-MSC or PBS group 1 day after MSC transplantation; neither FTH-positive nor blue-stained MSCs were observed in the glioma margin zone.

On T2W images, GL261 gliomas appeared as hyperintense masses commonly surrounded by hypointense hemorrhage (figure 3A). In vivo MRI (figure 3A) and tumor volume growth curves (figure 3B) showed that the CXCL10-Nrf2-FTH-MSC and CXCL10-FTH-MSC groups

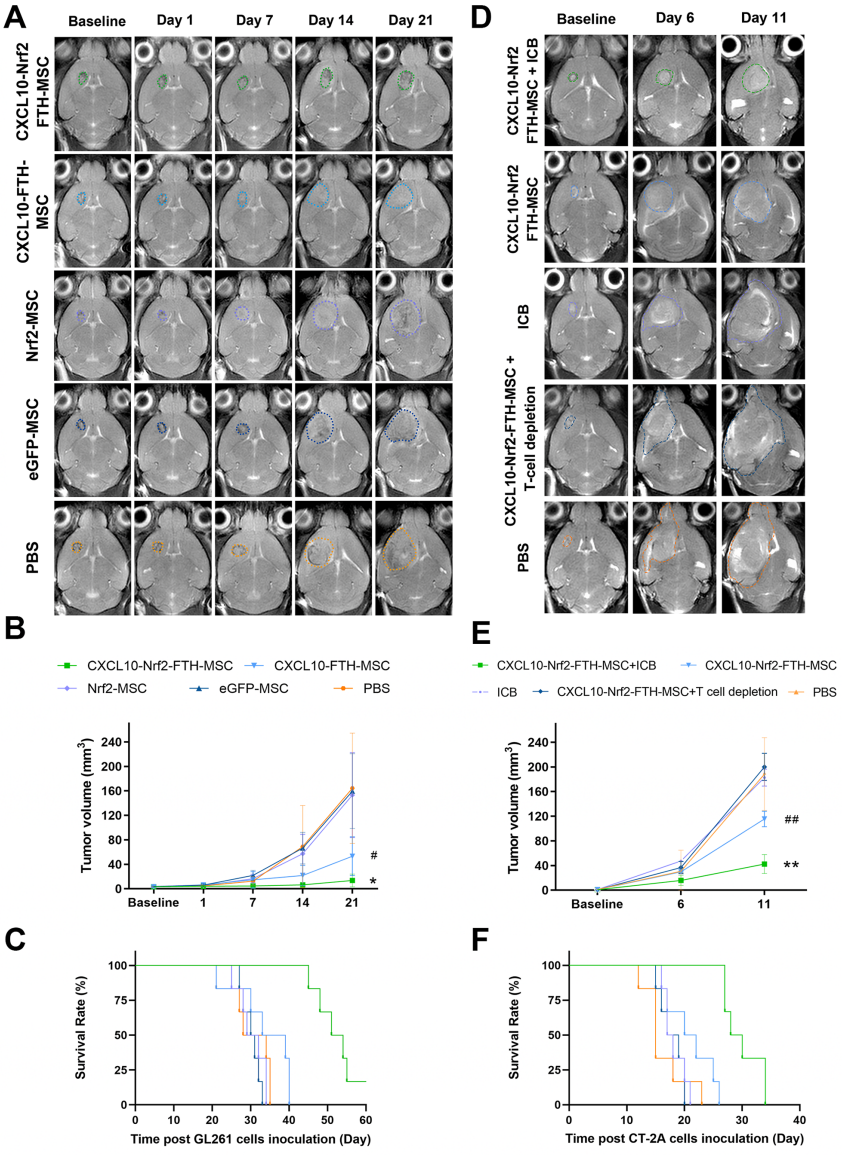

Figure 3 In vivo MRI monitoring and survival analyses for GL261 and CT2A GBMs. (A) On T2W images, GL261 tumors are depicted as masses with a hyperintense signal that are frequently accompanied by hypointense hemorrhage. From baseline to day 21, GL261 tumors receiving the CXCL10-Nrf2-FTH-MSCs treatment revealed a slower development pattern than those receiving other therapies. (B) Tumor growth curves reveal CXCL10-Nrf2-FTH-MSCs exhibited the lowest rate of tumor development. The tumor growth rate of the CXCL10-FTH-MSC group was intermediate between that of the CXCL10-Nrf2-FTH-MSC group and the control groups. (C) Kaplan-Meier survival analysis shows that mice in the CXCL10-Nrf2-FTH-MSC group lived considerably longer than the other four groups ($p<0.001$), and the CXCL10-FTH-MSC group also lived longer than the Nrf2-MSC, eGFP-MSC, and PBS groups ($p>0.05$). According to in vivo MRI (D) and tumor growth curves (E) CT2A tumors in the CXCL10-Nrf2-FTH-MSC + ICB group grew at the slowest rate relative to the other four groups ($p<0.01$), while CT2A tumors in the CXCL10-Nrf2-FTH-MSC group also grew more slowly than the ICB group, CXCL10-Nrf2-FTH-MSC + T-cell depletion group, and PBS group ($p<0.05$). (F) Kaplan-Meier survival analysis shows that mice with CT2A GBMs in the CXCL10-Nrf2-FTH-MSC + ICB group had significantly improved survival than the other four groups. ($^{\#}$: CXCL10-FTH-MSC vs Nrf2-MSC, eGFP-MSC, PBS, $p<0.05$; *: CXCL10-Nrf2-FTH-MSC vs Nrf2-MSC, eGFP-MSC, PBS, $p<0.05$; $^{\#\#}$: CXCL10-Nrf2-FTH-MSC vs ICB, CXCL10-Nrf2-FTH-MSC + T cell-depletion, PBS, $p<0.05$; **: CXCL10-Nrf2-FTH-MSC + ICB vs CXCL10-Nrf2-FTH-MSC, ICB, CXCL10-Nrf2-FTH-MSC + T cell-depletion, PBS, $p<0.05$). eGFP, enhanced green fluorescent protein; GBM, glioblastoma; ICB, immune checkpoint blockade; MSCs, mesenchymal stem cells.

showed significantly slower tumor growth than the other groups ($p<0.05$). Comparatively, the tumor volume of the CXCL10-Nrf2-FTH-MSC group ($13.68\pm10.35\,mm^3$) is significantly less than that of the CXCL10-FTH-MSC group ($53.30\pm31.62\,mm^3$) ($p<0.05$) on day 21. The mice in the Nrf2-MSC and eGFP-MSC groups all displayed the same pattern of progressive tumor growth as the PBS group ($p>0.05$). According to the Kaplan-Meier survival analysis (figure 3C), mice in the CXCL10-Nrf2-FTH-MSC group had significantly longer survival (median survival time:

52.5 days) than the other four groups (median survival time: 30.5–36 days) ($p<0.05$); 66.7% (4/6) animals in the CXCL10-Nrf2-FTH-MSC group survived for 50 days. The mice in the CXCL10-FTH-MSC group lived longer than the Nrf2-MSC, eGFP-MSC, and PBS groups, but there was no statistically significant difference ($p>0.05$) (figure 3C). These findings indicated that peritumoral injection of CXCL10-Nrf2-FTH-MSCs significantly inhibited GL261 tumor growth and extended animal survival, while CXCL10-FTH-MSCs exhibited a comparatively moderate therapeutic effect on GL261 tumors.

To validate the therapeutic efficacy, CT2A GBMs, which are immunologically inert and more analogous to human GBM than GL261 gliomas,[23 24] were used. As determined by in vivo MRI (figure 3D) and tumor volume growth curves (figure 3E), peritumoral transplantation of CXCL10-Nrf2-FTH-MSCs substantially slowed tumor growth. Survival analysis (figure 3F) showed an improvement in survival for mice in the CXCL10-Nrf2-FTH-MSC group (median survival time: 21 days) compared to the PBS group (median survival time: 15 days), with a marginally significant difference ($p=0.081$). Notably, mice bearing CT2A GBM in the CXCL10-Nrf2-FTH-MSC + ICB group exhibited a significantly slower rate of tumor growth ($p<0.01$) and considerably prolonged survival in comparison to the other four groups ($p<0.001$). In contrast, single ICB therapy or CXCL10-Nrf2-FTH-MSC transplantation after T-cell depletion did not yield a significant effect on the growth of CT2A tumors or the survival of the animals. These results suggest that the therapeutic efficacy of CXCL10-Nrf2-FTH-MSCs against CT2A tumors was amplified when in combination with ICB therapy.

Histology assesses CXCL10-Nrf2-FTH-MSC survival, CXCL10 secretion, and GBM cell proliferation and apoptosis after transplantation

Immunofluorescence imaging of eGFP (figure 4A) revealed abundant $eGFP^+$ cells in the marginal region of the tumor in the CXCL10-Nrf2-FTH-MSC and Nrf2-MSC groups on day 7 after transplantation, and considerable $eGFP^+$ cells were still detected for these two groups within the tumor on day 21 after transplantation. On day 7 after transplantation, the tumor contained a number of $eGFP^+$ cells in both the CXCL10-FTH-MSC and eGFP-MSC groups. Neither the CXCL10-FTH-MSC group nor the eGFP-MSC group contained $eGFP^+$ cells on day 21 following transplantation. Quantitative analysis (figure 4B) showed that on day 7 after transplantation, the proportion of $eGFP^+$ cells in the CXCL10-Nrf2-FTH-MSC group was significantly higher (83%±4.41%) than that in the CXCL10-FTH-MSC group (36.48%±6.65%), Nrf2-MSC group (55.75%±7.20%), and eGFP-MSC group (29.94%±5.25%) ($p<0.05$). By day 21, the proportion of $eGFP^+$ cells in the CXCL10-Nrf2-FTH-MSC group had declined to 49.17%±9.84%, but remained significantly higher than that in the Nrf2 group (29.67%±5.44%) and in the CXCL10-FTH-MSC and eGFP-MSC groups (both around 1%) ($p<0.01$). The Nrf2-MSC group showed more $eGFP^+$ cells than the CXCL10-FTH-MSC and eGFP-MSC groups on both day 7 and day 21 ($p<0.001$). These results indicate that Nrf2-overexpressing MSCs have a greater capacity for survival following glioma transplantation.

On days 7 and 21 after MSC transplantation, the CXCL10 levels in brain tissue of the CXCL10-Nrf2-FTH-MSC group were significantly higher than those of the other four groups ($p<0.05$) (figure 4C). Only on day 7 did the CXCL10-FTH-MSC group exhibit a significantly higher CXCL10 level in comparison to the Nrf2-MSC, eGFP-MSC, and PBS groups ($p<0.05$). The levels of CXCL10 were not significantly upregulated in the Nrf2-MSC, eGFP-MSC, and PBS groups. These findings suggest that CXCL10-Nrf2-FTH-MSCs with a longer lifespan secrete more CXCL10 into the tumor.

On both day 7 and day 21 following transplantation, TUNEL staining (figure 4D) revealed a significantly greater number of apoptotic tumor cells in the CXCL10-Nrf2-FTH-MSC group than in the other four groups. Ki67 immunohistochemical staining (figure 4E) revealed that on days 7 and 21 after transplantation, in comparison to the other four groups, GBMs treated with CXCL10-Nrf2-FTH-MSCs displayed considerably decreased Ki67 expression. These findings suggest that peritumoral transplantation of CXCL10-Nrf2-FTH-MSCs promotes apoptosis and inhibits proliferation in GBM cells.

CXCL10-Nrf2-MSC increase tumor-infiltrating $CD8^+$ T lymphocytes and rescue T-cell dysfunction

Day 7 after MSC transplantation showed a significant increase in $CD8^+$ T cells (figure 5A), IFN-γ^+ cytotoxic T lymphocytes (CTLs) (figure 5B), $GzmB^+$ CTLs (figure 5C), and Th1 cells (figure 5D) and a significant decrease in Treg cells (figure 5E) in the GL261 tumors treated with CXCL10-Nrf2-FTH-MSCs or CXCL10-FTH-MSCs compared with those treated by the Nrf2-MSC, eGFP-MSC, or PBS ($p<0.05$). On day 21 after MSC transplantation, only GL261 tumors treated with CXCL10-Nrf2-FTH-MSCs demonstrated a significant increase in $CD8^+$ T cells, IFN-γ^+ CTLs, $GzmB^+$ CTLs, and Th1 cells ($p<0.05$). Transplanting Nrf2-MSCs and eGFP-MSCs did not substantially change the immune cells in TME on both days 7 and 21. These results suggest that CXCL10-Nrf2-FTH-MSCs exert a long-term anti-GBM effect not only by increasing the trafficking of $CD8^+$ T cells to the tumor site but also by directing $CD8^+$ T cells and $CD4^+$ T cells into highly potent effector T cells and altering the immunosuppressive immunological milieu.

It has been demonstrated that the CXCR3-CXCL10 axis regulates T lymphocyte migration and activation.[25] To determine the alteration in the CXCR3-CXCL10 axis, $CXCR3^+$ cells were analyzed by FCM in both the tumor and dCLNs. We found that the CXCL10-Nrf2-FTH-MSC and CXCL10-FTH-MSC groups had more $CXCR3^+$ cells in dCLNs and GL261 tumors than the Nrf2-MSC, eGFP-MSC, and PBS groups on day 7 after MSC transplantation ($p<0.05$) (online supplemental figure S4). Moreover, the CXCL10-Nrf2-FTH-MSC group had

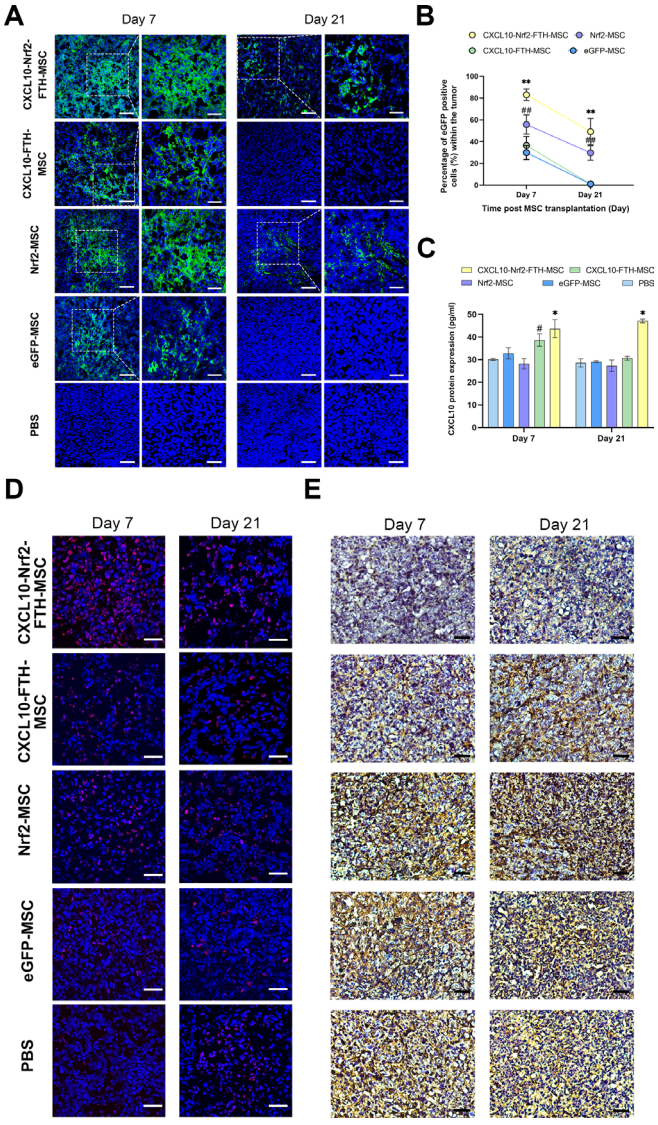

Figure 4 CXCL10-Nrf2-FTH-MSC survival, CXCL10 Secretion, and therapeutic effect on glioblastoma. (A) Representative micrographs of eGFP immunofluorescence demonstrate that a large number of eGFP$^+$ cells could be identified on day 7 after transplantation in the CXCL10-Nrf2-FTH-MSC and Nrf2-MSC groups, and considerable eGFP$^+$ cells could still be observed on day 21 following transplantation. Only on day 7 after transplantation did the CXCL10-FTH-MSC and eGFP-MSC groups show eGFP$^+$ cells. Twenty-one days after transplantation, neither the CXCL10-FTH-MSC nor the eGFP-MSC group contained eGFP$^+$ cells. (Bar=100 µm, 50 µm). (B) On day 21, except for the CXCL10-Nrf2-FTH-MSC and Nrf2-MSC groups, the percentage of eGFP$^+$ cells in the CXCL10-FTH-MSC, eGFP-MSC, and PBS groups decreased to nearly zero. (C) After peritumoral transplantation of CXCL10-Nrf2-FTH-MSCs on both days 7 and 21, the level of CXCL10 secretion in the brain tissues of tumor-bearing animals was elevated. In the CXCL10-FTH-MSC group, CXCL10 secretion was considerably higher than in the Nrf2-MSC, eGFP-MSC, and PBS groups only on day 7 after transplantation; on day 21 after transplantation, it recovered to a level comparable to the eGFP-MSC and PBS groups. (D) TUNEL stains show that on days 7 and 21 after transplantation, there were more apoptotic tumor cells detected in the CXCL10-Nrf2-FTH-MSC group than in any of the other four groups. (Bar=50 µm). (E) Representative Ki67 immunohistochemical micrographs for gliomas show Ki67 expression was lowest in the CXCL10-Nrf2-FTH-MSC group on days 7 and 21 after injection, followed by the CXCL10-FTH-MSC group, and higher in the Nrf2-MSC, eGFP-MSC, and PBS groups. (Bar=40 µm). ($^{\#}$: CXCL10-FTH-MSC vs Nrf2-MSC, eGFP-MSC, PBS, $p<0.05$; *: CXCL10-Nrf2-FTH-MSC vs CXCL10-FTH-MSC, Nrf2-MSC, eGFP-MSC, PBS, $p<0.05$; $^{\#\#}$: Nrf2-MSC vs CXCL10-FTH-MSC, eGFP-MSC, $p<0.05$; **: CXCL10-Nrf2-FTH-MSC vs CXCL10-FTH-MSC, Nrf2-MSC, eGFP-MSC, $p<0.05$). eGFP, enhanced green fluorescent protein; MSCs, mesenchymal stem cells.

more CXCR3$^+$ cells in GL261 tumors than the CXCL10-FTH-MSC group did on day 7 ($p<0.001$). On day 21, only the CXCL10-Nrf2-FTH-MSC group showed more CXCR3$^+$ cells in GL261 tumors than the other four groups ($p<0.05$), with no significant differences in dCLN CXCR3$^+$ cells among all groups ($p>0.05$) (online supplemental figure S4). These results indicate that CXCL10-Nrf2-FTH-MSC transplantation enhances CXCR3$^+$ lymphocyte activation in dCLNs and CXCR3$^+$ lymphocyte migration into GBMs.

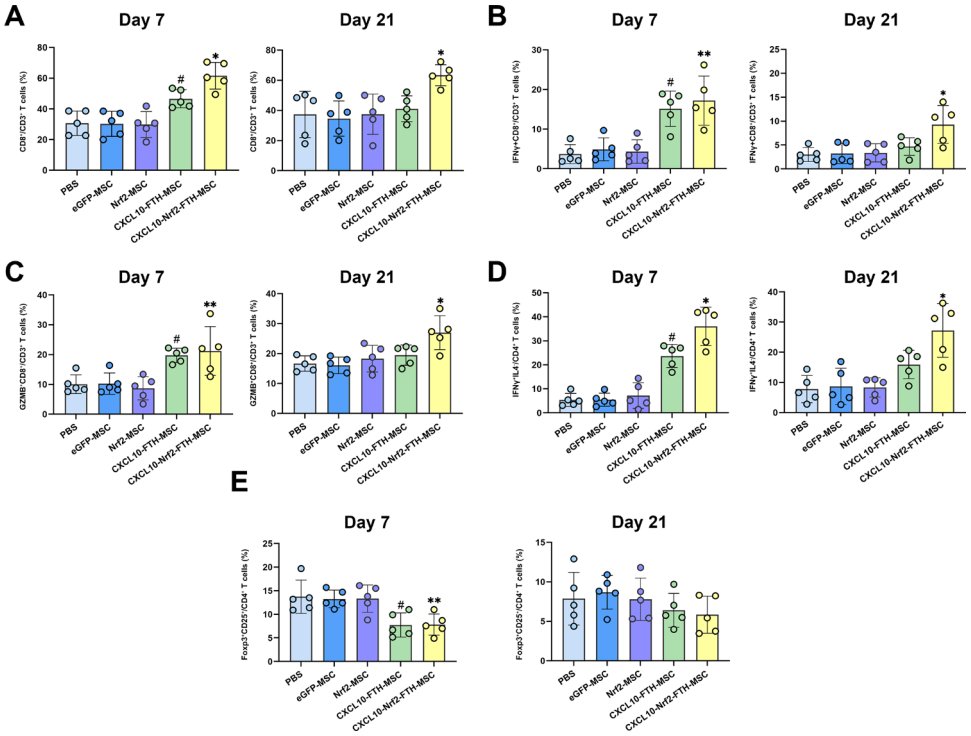

Figure 5 Flow cytometry analysis of T lymphocyte subsets in the GL261 tumors 7 days and 21 days after MSC transplantation On day 7 after MSC transplantation, significant increases in $CD8^+$ T cells (A) IFN-γ^+ CTLs (B) $GzmB^+$ CTLs (C) and Th1 cells (D) were observed in the GL261 tumors treated with CXCL10-Nrf2-FTH-MSCs or CXCL10-FTH-MSCs, while Treg cells (E) decreased significantly, in comparison to the Nrf2-MSC, eGFP-MSC, and PBS groups ($p<0.05$). On day 21, only GL261 tumors in the CXCL10-Nrf2-FTH-MSC group exhibited a statistically significant increase in $CD8^+$ T cells (A) IFN-γ^+ CTLs (B) $GzmB^+$ CTLs (C) and Th1 cells (D) ($p<0.05$). ($^{\#}$: CXCL10-FTH-MSC vs Nrf2-MSC, eGFP-MSC, PBS, $p<0.05$; *: CXCL10-Nrf2-FTH-MSC vs CXCL10-FTH-MSC, Nrf2-MSC, eGFP-MSC, PBS, $p<0.05$; **: CXCL10-Nrf2-FTH-MSC vs Nrf2-MSC, eGFP-MSC, PBS, $p<0.05$). CTL, cytotoxic T lymphocyte; eGFP, enhanced green fluorescent protein; IFN, interferon; IL, interleukin; MSCs, mesenchymal stem cells; Treg, regulatory T cell.

Ex vivo FCM in CT2A GBMs revealed that the CXCL10-Nrf2-FTH-MSC + T-cell depletion group showed almost no $CD8^+$ T cells (0.33±0.18%) (figure 6A); therefore, more in-depth analyses of T-cell phenotype were not performed for this group. CT2A GBMs in the CXCL10-Nrf2-FTH-MSC + ICB and CXCL10-Nrf2-FTH-MSC groups showed a significant increase in $CD8^+$ T cells (figure 6A), IFN-γ^+ CTLs (figure 6B), $GzmB^+$ CTLs (figure 6C), along with a notable decrease in Treg (figure 6E), exhausted $CD8^+$ T lymphocytes (figure 6F), and exhausted $CD4^+$ T lymphocytes (figure 6G) when compared with the ICB and PBS groups ($p<0.05$). Furthermore, the CXCL10-Nrf2-FTH-MSC + ICB group showed more $CD8^+$ T cells, IFN-γ^+ CTLs, and $GzmB^+$ CTLs than the CXCL10-Nrf2-FTH-MSC group ($p<0.05$), and only the CXCL10-Nrf2-FTH-MSC + ICB group had a higher level of Th1 cells (figure 6D) compared with the other three groups ($p<0.05$). There were no significant differences between the ICB and PBS groups in any of the indices ($p>0.05$). No significant changes were found for tumor-associated M1 macrophages (figure 6H) and M2 macrophages (figure 6I) across all groups ($p>0.05$). These results show ICB therapy alone cannot change the TME of CT2A GBM, but CXCL10-Nrf2-FTH-MSCs could restore T-cell dysfunction in CT2A GBM, and ICB therapy could enhance this capacity further.

DISCUSSION

In this study, we constructed genetically modified CXCL10-Nrf2-FTH-MSCs with increased T lymphocyte recruitment, tolerance to oxidative stress, and iron accumulation. Under in vivo FTH-MRI guidance and surveillance, peritumoral transplantation of CXCL10-Nrf2-FTH-MSCs inhibited orthotopic GL261 and CT2A GBM tumor growth in C57/BL6 mice and prolonged mouse survival. When combined with ICB therapy, the therapeutic benefit of CXCL10-Nrf2-FTH-MSCs for CT2A GBM could be enhanced. Histology analyses demonstrated that peritumorally administered CXCL10-Nrf2-FTH-MSCs survived longer in the TME, enhanced CXCL10 production, and ultimately inhibited GBM growth by enhancing tumor-infiltrating T cells and restoring T-cell function. Our findings were summarized in figure 7.

In 2015, Louveau *et al* disproved the conventional belief that the CNS is an "immune-privileged" region and opened the door to the immunotherapeutic treatment of GBM by demonstrating that meningeal lymphatic

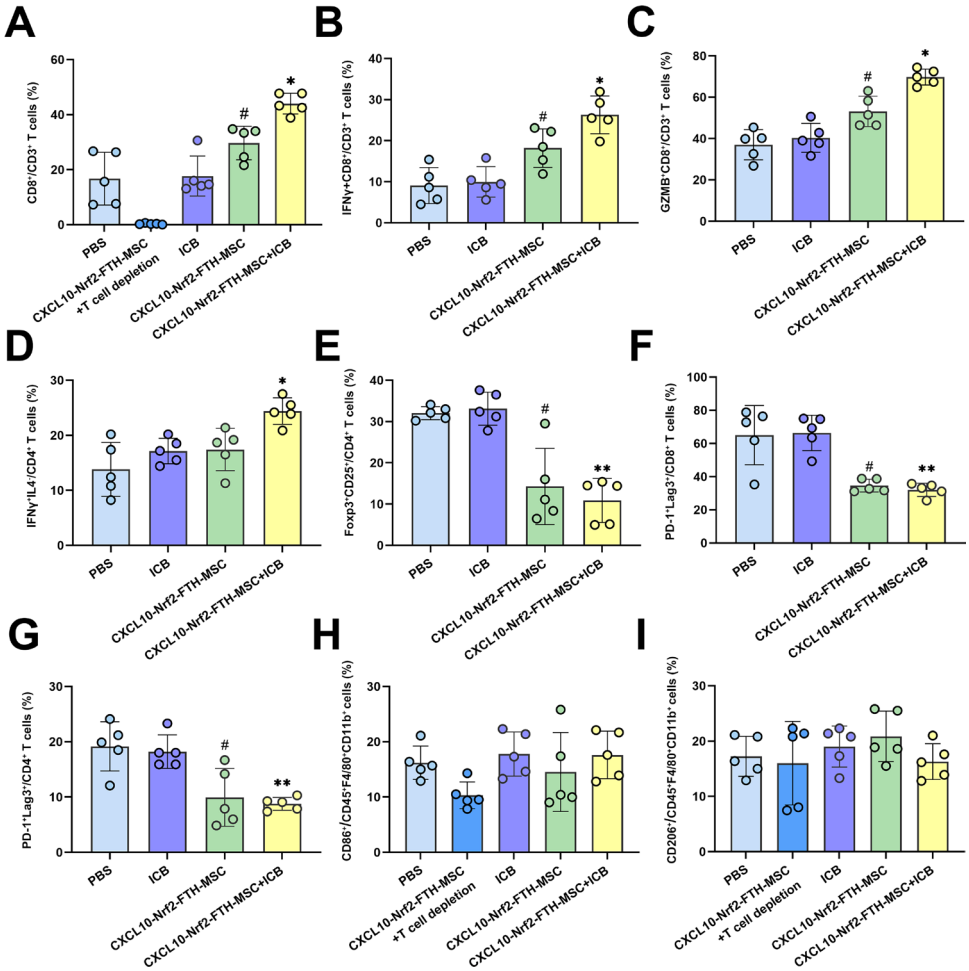

Figure 6 Flow cytometry analysis of lymphocyte subsets of CT2A GBMs. Compared with the ICB and PBS groups, CT2A GBMs in the CXCL10-Nrf2-FTH-MSC + ICB and CXCL10-Nrf2-FTH-MSC groups exhibited a statistically significant increase in $CD8^+$ T cells (A) IFN-γ^+ CTLs (B) and $GzmB^+$ CTLs (C) whereas Treg (E) exhausted $CD8^+$ T lymphocytes (F) and exhausted $CD4^+$ T lymphocytes (G) were significantly lower ($p<0.05$). In addition, the CXCL10-Nrf2-FTH-MSC + ICB group exhibited a greater quantity of $CD8^+$ T cells (A) IFN-γ^+ CTLs (B) and $GzmB^+$ CTLs (C) in comparison to the CXCL10-Nrf2-FTH-MSC group ($p<0.05$). Only the CXCL10-Nrf2-FTH-MSC + ICB group exhibited a greater percentage of Th1 cells (D) across the groups ($p<0.05$). No significant changes were found for tumor-associated M1 macrophages (G) and M2 macrophages (H) across all groups ($p>0.05$). (#: CXCL10-Nrf2-FTH-MSC vs ICB, PBS, $p<0.05$; *: CXCL10-Nrf2-FTH-MSC + ICB vs CXCL10-Nrf2-FTH-MSC, ICB, PBS, $p<0.05$; **: CXCL10-Nrf2-FTH-MSC + ICB vs ICB, PBS, $p<0.05$). CTL, cytotoxic T lymphocyte; eGFP, enhanced green fluorescent protein; GBM, glioblastoma; ICB, immune checkpoint blockade; IFN, interferon; IL, interleukin; MSCs, mesenchymal stem cells; PD-1, programmed cell death-1; Treg, regulatory T cell.

drainage between the brain parenchyma and dCLNs is crucial for immunological monitoring of the CNS.[26] Our research revealed an increase in $CXCR3^+$ lymphocyte activation in dCLNs and $CXCR3^+$ lymphocyte infiltration in the GBMs in response to CXCL10-Nrf2-FTH-MSC transplantation, indicating the existence of communication between dCLNs and brain tumors as well as the importance of the CXCR3-CXCL10 axis in the regulation of T lymphocytes, as previously reported.[25] Based on current observations, immunotherapies such as PD-1/programmed death-ligand 1 (PD-L1) blockade, CAR T-cell therapy, oncolytic virus therapy, and peptide or dendritic cell vaccines have so far failed to yield a meaningful survival benefit for patients with GBM in phase III clinical trials.[4] Current research in the field has demonstrated that this failure can be due to the unique immunological milieu of brain tumors, which is characterized by a deficiency of T lymphocytes and an abundance of immune suppressors that render T cells dysfunctional.[27] In the current study, gene-modified MSCs that overexpress CXCL10 were transplanted into orthotopic intracranial GBM in mice. Not only did CXCL10-Nrf2-FTH-MSCs enhance $CD8^+$ T lymphocytes infiltrating the tumor, but it also reprogrammed $CD8^+$ T cells and $CD4^+$ T cells into tumor-suppressing $GzmB^+$CTLs, IFN-γ^+ CTLs and Th1 cells, while decreasing Treg, exhausted $CD8^+$ and exhausted $CD4^+$ T cells. This outcome is consistent with earlier studies. Rosa Barreira da Silva *et al* provided direct in vivo evidence that higher concentrations of CXCL10 correspond with significantly increased trafficking of $CD8^+$ T cells into the melanoma.[28] Peng *et al* demonstrated that treatment with epigenetic modulators such as DNA methyltransferase

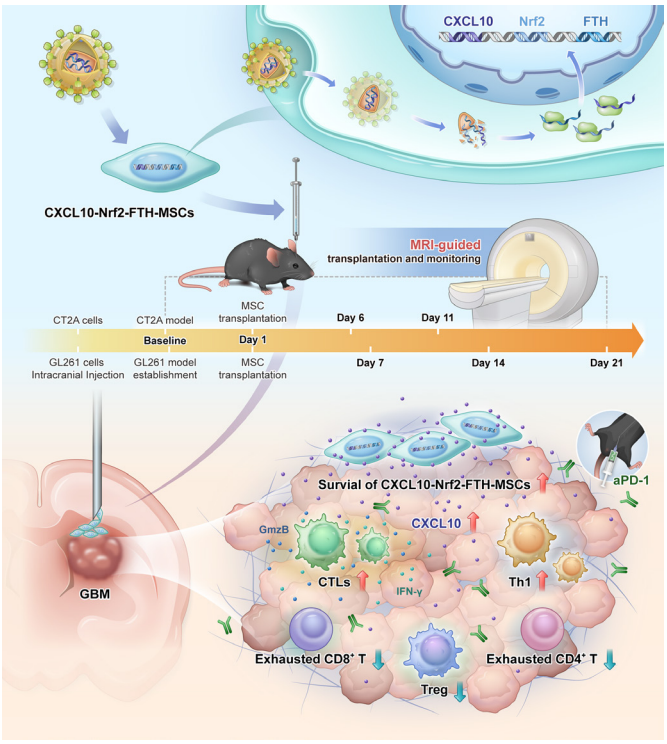

Figure 7 Schematic illustration of MRI-guided peritumoral administration of CXCL10 and Nrf2 upregulated mesenchymal stem cells reinvigorates T lymphocytes in GBM. aPD-1, anti-programmed cell death-1 antibody; CTL, cytotoxic T lymphocyte; GBM, glioblastoma; IFN, interferon; MSC, mesenchymal stem cell; Treg, regulatory T cell.

and histone deacetylase inhibitors promoted tumor production of CXCL10, which resulted in increased effector T-cell tumor infiltration and slowed the progression of ovarian cancer.[29] Notably, consistent with earlier studies, this study found that ICB therapy alone had no therapeutic impact on CT2A GBM, an immunologically inert GBM model that is more similar to human GBM than GL261 model.[23 24] Nonetheless, the therapeutic efficacy of CXCL10-Nrf2-FTH-MSCs against CT2A tumors could be enhanced when combined with ICB therapy. This result is consistent with Peng *et al*'s research,[30] which suggests that inhibiting the PD-1 pathway can upregulate IFN-γ and CXCL10 at the tumor site, potentially initiating a positive feedback loop through the CXCL10/CXCR3 axis. All of these findings indicated that peritumoral CXCL10-Nrf2-FTH-MSC transplantation could inhibit GBM growth by revitalizing T lymphocytes in the TME, and this ability could be enhanced when combined with ICB therapy, providing a promising method for treating immunologically "distinct" GBM.

MSCs could be employed as cellular vehicles to deliver CXCL10 to GBM. However, the low lifespan of donated stem cells in tumors is a major roadblock to tumoricidal stem cell treatment.[31] Our previous studies have demonstrated that the vast majority of implanted MSCs perish during the first several days after administration, severely limiting their therapeutic potential against GBM.[14 32] To overcome this limitation, hydrogels or electrospun scaffolds have been used to encapsulate tumoricidal stem cells, thereby extending their persistence in the brain and enhancing their therapeutic efficacy against GBM.[33] However, due to increased intracranial pressure, polymeric biomaterial scaffolds containing tumoricidal stem cells are mostly used in post-surgical GBMs.[33] To circumvent this problem, genetic engineering MSCs with anti-apoptotic genes such as Hif-1α,[34] Bcl-2,[35] and H2AX[36] can improve MSCs' resistance to the cytotoxic microenvironment, thereby enhancing MSCs' survival and their therapeutic efficacy for ischemic stroke, myocardial infarction, and Parkinson's disease. Recent research has established that pharmacological activation of Nrf2 increases the response of MSCs to various stressors, such as hypoxia, oxidative stress, excessive nutrient and metabolite supply, etc.[16] As TME is characterized by an aberrant oxygen metabolism and elevated levels of ROS,[37] MSCs were genetically engineered to overexpress Nrf2. Our research shows that Nrf2 overexpression improves MSC tolerance to oxidative stress and increases their ability to survive following transplantation into GBMs. These results suggest that Nrf2 overexpression in MSCs is a feasible strategy for enhancing MSC survival and serving as a cellular carrier for GBM.

It has been demonstrated that the route of stem cell delivery has a significant impact on therapeutic benefit.[38] In a prior study, we demonstrated that peritumoral injection is the optimum transplantation method for INF-β-MSCs against intracranial orthotopic glioma, as compared with intracerebral, intratumoral, or intra-arterial injection.[14] To achieve precise transplantation into the tumor periphery, MSCs were transduced with lentiviral vectors expressing the *Fth* reporter gene and administered under the guidance of FTH-MRI in the present study. Histological examinations confirmed the implantation of MSCs in the GBM periphery. MRI-guided technology is a reliable approach for delivering genes to the correct anatomical target in the brain.[39] Previously, Pearson *et al* developed an MR-guided gene delivery platform for the administration of adeno-associated virus vectors to the midbrain in children with aromatic L-amino acid decarboxylase deficiency.[40] Our research showed that FTH-MRI is a feasible technique for guiding stem cell transplantation for intracranial glioma, suggesting its broader application in cellular therapy for diseases of the brain.

Our study has some drawbacks. First, only peritumoral injection was chosen as the administration route for CXCL10-Nrf2-FTH-MSC delivery in this study. Our previous study has demonstrated that only peritumoral injection of IFN-β-upregulated MSCs exerts a therapeutic effect in a rat model of intracranial orthoptic glioma, while intracerebral, intratumoral, and intra-arterial injections of IFN-β-upregulated MSCs have no beneficial effect.[14] Given the fact that MSCs transplanted into the contralateral hemisphere could migrate towards the glioma along the corpus callosum from the initial injection site,[41] future investigations are needed to determine

whether CXCL10-Nrf2-FTH-MSC injected contralaterally into the brain parenchyma could inhibit GBM. Second, although FTH-MRI could be used to track the migration and distribution of transplanted MSCs, it is challenging to monitor their viability inside the tumor. Because hypointense signals on T2W images are not specific to MSCs labeled with FTH, they may also result from the frequent intratumoral hemorrhage observed in GBMs. In the future, diffusion-based MRI reporter genes such as aquaporin 1[42] or chemical exchange saturation transfer (CEST) MRI-based reporter genes such as lysine-rich protein[43] may enhance the differentiation between viable cells and endogenous hemorrhage.

In conclusion, our study demonstrated that peritumoral administration of CXCL10 and Nrf2-overexpressed MSCs can significantly limit GBM growth by reinvigorating T lymphocytes within the TME, hence providing a therapeutic option for malignant gliomas. Combining CXCL10-Nrf2-FTH-MSC transplantation with ICB therapy can potentially be an effective treatment regimen for GBM.

Contributors JM and JL conducted the main experiments and wrote the manuscript. JC established the animal models. QW performed mesenchymal stem cell transduction. MC guided medical imaging. FZ assisted with pathological examinations. BL contributed to data interpretation. QZ and ZW assisted with in vitro experiments. JZ designed the lentiviral vector. JS supervised the study. All authors read and approved the final version of the manuscript. JS is responsible for the overall content as guarantor.

Funding This study was supported by the National Natural Science Foundation of China (Grant no. 82001768, and 82171996), Guangdong Natural Science Foundation (Grant no. 2021A1515010226, 2022A1515010279), and National Key R&D Program of China (Grant No. 2022YFA1104800).

Competing interests None declared.

Patient consent for publication Not applicable.

Ethics approval The Ruige Biotechnology Institutional Animal Care and Use Committee (Guangzhou, China) granted its approval for all mouse studies in our investigation (Approval No. 20211201-001), which were carried out in accordance with their guidelines for the care and use of laboratory animals.

Provenance and peer review Not commissioned; externally peer reviewed.

Data availability statement Data are available upon reasonable request.

ORCID iD

Jun Shen http://orcid.org/0000-0001-7746-5285

REFERENCES

1 Tan AC, Ashley DM, López GY, *et al*. Management of glioblastoma: state of the art and future directions. *CA Cancer J Clin* 2020;70:299–312.
2 Stupp R, Taillibert S, Kanner A, *et al*. Effect of tumor-treating fields plus maintenance temozolomide vs maintenance temozolomide alone on survival in patients with glioblastoma: a randomized clinical trial. *JAMA* 2017;318:2306–16.
3 Schaff LR, Mellinghoff IK. Glioblastoma and other primary brain malignancies in adults: A review. *JAMA* 2023;330:189–90.
4 McGranahan T, Therkelsen KE, Ahmad S, *et al*. Current state of immunotherapy for treatment of glioblastoma. *Curr Treat Options Oncol* 2019;20:24.
5 Medikonda R, Dunn G, Rahman M, *et al*. A review of glioblastoma immunotherapy. *J Neurooncol* 2021;151:41–53.
6 Rahman M, Sawyer WG, Lindhorst S, *et al*. Adult Immuno-oncology: using past failures to inform the future. *Neuro Oncol* 2020;22:1249–61.
7 Chow MT, Ozga AJ, Servis RL, *et al*. Intratumoral activity of the CXCR3 Chemokine system is required for the efficacy of anti-PD-1 therapy. *Immunity* 2019;50:1498–512.
8 Mikucki ME, Fisher DT, Matsuzaki J, *et al*. Non-redundant requirement for CXCR3 signalling during tumoricidal T-cell trafficking across tumour vascular checkpoints. *Nat Commun* 2015;6:7458.
9 Barash U, Zohar Y, Wildbaum G, *et al*. Heparanase enhances myeloma progression via CXCL10 downregulation. *Leukemia* 2014;28:2178–87.
10 Attia N, Mashal M, Pemminati S, *et al*. Cell-based therapy for the treatment of glioblastoma: an update from preclinical to clinical studies. *Cells* 2021;11:116.
11 Zhang Q, Xiang W, Yi D-Y, *et al*. Current status and potential challenges of mesenchymal stem cell-based therapy for malignant gliomas. *Stem Cell Res Ther* 2018;9:228.
12 Fares J, Ahmed AU, Ulasov IV, *et al*. Neural stem cell delivery of an oncolytic adenovirus in newly diagnosed malignant glioma: a first-in-human, phase 1, dose-escalation trial. *Lancet Oncol* 2021;22:1103–14.
13 Binello E, Germano IM. Stem cells as therapeutic vehicles for the treatment of high-grade gliomas. *Neuro Oncol* 2012;14:256–65.
14 Mao J, Cao M, Zhang F, *et al*. Peritumoral administration of IFNβ upregulated mesenchymal stem cells inhibits tumor growth in an orthotopic, immunocompetent rat glioma model. *J Immunother Cancer* 2020;8:e000164.
15 Holmström KM, Finkel T. Cellular mechanisms and physiological consequences of redox-dependent signalling. *Nat Rev Mol Cell Biol* 2014;15:411–21.
16 Dai X, Yan X, Wintergerst KA, *et al*. Nrf2: redox and metabolic regulator of stem cell state and function. *Trends Mol Med* 2020;26:185–200.
17 Mohammadzadeh M, Halabian R, Gharehbaghian A, *et al*. Nrf-2 overexpression in mesenchymal stem cells reduces oxidative stress-induced apoptosis and cytotoxicity. *Cell Stress Chaperones* 2012;17:553–65.
18 Yuan Z, Zhang J, Huang Y, *et al*. Nrf2 overexpression in mesenchymal stem cells induces stem-cell marker expression and enhances Osteoblastic differentiation. *Biochem Biophys Res Commun* 2017;491:228–35.
19 Khan SM, Desai R, Coxon A, *et al*. Impact of Cd4 T cells on Intratumoral Cd8 T-cell exhaustion and responsiveness to PD-1 blockade therapy in Mouse brain tumors. *J Immunother Cancer* 2022;10:e005293.
20 Woroniecka KI, Rhodin KE, Dechant C, *et al*. 4-1Bb Agonism averts TIL exhaustion and licenses PD-1 blockade in glioblastoma and other intracranial cancers. *Clin Cancer Res* 2020;26:1349–58.
21 Pandey V, Fleming-Martinez A, Bastea L, *et al*. Cxcl10/Cxcr3 signaling contributes to an inflammatory Microenvironment and its blockade enhances progression of murine Pancreatic precancerous lesions. *Elife* 2021;10:e60646.
22 Loubaki L, Tremblay T, Bazin R. In vivo depletion of leukocytes and platelets following injection of T cell-specific antibodies into mice. *J Immunol Methods* 2013;393:38–44.
23 Khalsa JK, Cheng N, Keegan J, *et al*. Immune phenotyping of diverse syngeneic murine brain tumors identifies Immunologically distinct types. *Nat Commun* 2020;11:3912.
24 Liu CJ, Schaettler M, Blaha DT, *et al*. Treatment of an aggressive orthotopic murine glioblastoma model with combination checkpoint blockade and a multivalent Neoantigen vaccine. *Neuro Oncol* 2020;22:1276–88.
25 Tokunaga R, Zhang W, Naseem M, *et al*. CXCL9, CXCL10, CXCL11/CXCR3 axis for immune activation - a target for novel cancer therapy. *Cancer Treat Rev* 2018;63:40–7.

26 Louveau A, Smirnov I, Keyes TJ, *et al*. Corrigendum: structural and functional features of central nervous system lymphatic vessels. *Nature* 2016;533:278.
27 Quail DF, Joyce JA. The microenvironmental landscape of brain tumors. *Cancer Cell* 2017;31:326–41.
28 Barreira da Silva R, Laird ME, Yatim N, *et al*. Dipeptidylpeptidase 4 inhibition enhances lymphocyte trafficking, improving both naturally occurring tumor immunity and immunotherapy. *Nat Immunol* 2015;16:850–8.
29 Peng D, Kryczek I, Nagarsheth N, *et al*. Epigenetic silencing of Th1-type chemokines shapes tumour immunity and immunotherapy. *Nature* 2015;527:249–53.
30 Peng W, Liu C, Xu C, *et al*. PD-1 blockade enhances T-cell migration to tumors by elevating IFN-Γ inducible chemokines. *Cancer Res* 2012;72:5209–18.
31 Hansen K, Müller F-J, Messing M, *et al*. A 3-dimensional extracellular matrix as a delivery system for the transplantation of glioma-targeting neural stem/progenitor cells. *Neuro Oncol* 2010;12:645–54.
32 Cao M, Mao J, Duan X, *et al*. In vivo tracking of the tropism of mesenchymal stem cells to malignant gliomas using reporter gene-based MR imaging. *Int J Cancer* 2018;142:1033–46.
33 Moore KM, Murthy AB, Graham-Gurysh EG, *et al*. Polymeric biomaterial scaffolds for tumoricidal stem cell glioblastoma therapy. *ACS Biomater Sci Eng* 2020;6:3762–77.
34 Lv B, Li F, Han J, *et al*. Hif-1A overexpression improves transplanted bone mesenchymal stem cells survival in rat MCAO stroke model. *Front Mol Neurosci* 2017;10:80.
35 Li W, Ma N, Ong L-L, *et al*. Bcl-2 engineered MSCs inhibited apoptosis and improved heart function. *Stem Cells* 2007;25:2118–27.
36 Jiang P, Huang P, Yen S-H, *et al*. Genetic modification of H2Ax renders Mesenchymal Stromal cell-derived dopamine neurons more resistant to DNA damage and subsequent apoptosis. *Cytotherapy* 2016;18:1483–92.
37 Liou GY, Storz P. Reactive oxygen species in cancer. *Free Radic Res* 2010;44:479–96.
38 Li L, Jiang Q, Ding G, *et al*. Effects of administration route on migration and distribution of neural progenitor cells transplanted into rats with focal cerebral ischemia, an MRI study. *J Cereb Blood Flow Metab* 2010;30:653–62.
39 Salegio EA, Samaranch L, Kells AP, *et al*. Guided delivery of adeno-associated viral vectors into the primate brain. *Adv Drug Deliv Rev* 2012;64:598–604.
40 Pearson TS, Gupta N, San Sebastian W, *et al*. Gene therapy for aromatic L-amino acid decarboxylase deficiency by MR-guided direct delivery of AAV2-AADC to Midbrain dopaminergic neurons. *Nat Commun* 2021;12:4251.
41 Menon LG, Kelly K, Yang HW, *et al*. Human bone marrow-derived mesenchymal stromal cells expressing S-TRAIL as a cellular delivery vehicle for human glioma therapy. *Stem Cells* 2009;27:2320–30.
42 Mukherjee A, Wu D, Davis HC, *et al*. Non-invasive imaging using reporter genes altering cellular water permeability. *Nat Commun* 2016;7:13891.
43 Farrar CT, Buhrman JS, Liu G, *et al*. Establishing the Lysine-rich protein CEST reporter gene as a CEST MR imaging detector for oncolytic virotherapy. *Radiology* 2015;275:746–54.